Nuclear magnetic relaxation study of carbon-13 in di-pentyl phthalate

Nuclear magnetic relaxation study of carbon-13 in di-pentyl phthalate

W Suchanski, E Szczesniak and S Jurga

Institute of Physics, A Mickiewicz University, ulica Umultowska 85, 61-614 Poznan, Poland

Abstract. Spin–lattice relaxation times T_1 and nuclear Overhauser enhancement factors of chemically non-equivalent carbons in di-pentyl phthalate (DPP), a simple glass-forming liquid, are measured as functions of temperature. The analysis shows that the correlation function describing the overall molecular dynamics in DPP can be well described in terms of an asymmetric distribution of correlation times predicted by the Davidson–Cole model. The distribution parameters β of the successive chain carbons are derived and analysed in terms of internal motions occurring in DPP.

1. Introduction

The problem of side-chain dynamics has been the focus of considerable attention [1–3], and measurements of ^{13}C spin–lattice relaxation times and nuclear Overhauser enhancement (NOE) factors have proved to provide the basis of a versatile method for studying this problem for a variety of molecular systems, such as supercooled liquids, glasses, biomolecules, micelles, and polymers [4–7]. The understanding of global and local dynamical properties of these complex systems is of great relevance to basic aspects of theory and to many branches of materials sciences. In the present paper we use ^{13}C NMR techniques to study di-pentyl phthalate. The selection of the compound for the study was motivated by the fact that its simple molecular structure may allow us to understand how the transition from a fluid to a solid glass, which occurs gradually as a liquid is supercooled, affects different reorientational degrees of freedom. While many NMR studies performed on supercooled liquids examine the coupling between translational and rotational motion [8], such studies on internal reorientations in flexible molecules are limited. We have studied the spin–lattice relaxation times T_1 and the NOE factors for DPP covering a temperature range between 227 and 356.8 K. When analysing the results obtained, we used the general expressions for the ^{13}C T_1 and NOE, which hold for the intramolecular dipolar relaxation mechanism on condition of complete proton decoupling [9]:

$$\frac{1}{nT_1} = C[J_0(\omega_H - \omega_C) + 3J_1(\omega_C) + 6J_2(\omega_H + \omega_C)] \tag{1}$$

$$\text{NOE} = 1 + \frac{\gamma_H}{\gamma_C} \frac{6J_2(\omega_H + \omega_C) - J_0(\omega_H + \omega_C)}{J_0(\omega_H - \omega_C) + 3J_1(\omega_C) + 6J_2(\omega_H + \omega_C)} \tag{2}$$

where the relaxation constant $C = 0.1(\gamma_H \gamma_C \hbar / r^3)^2$, n is the number of hydrogen nuclei involved in relaxation of a given carbon, r is the carbon–hydrogen internuclear distance, γ_H and γ_C are the gyromagnetic ratios for hydrogen and carbon, and ω_H, ω_C are their Larmor frequencies.

It is apparent that T_1 and the NOE factors are sensitive to the form of the spectral density function $J(\omega)$. The simplest $J(\omega)$, which involves a single correlation time τ and describes the isotropic reorientation of the C–H interaction vector, is expressed by [10]

$$J(\omega) = \frac{\tau}{1 + \omega^2\tau^2}. \tag{3}$$

The reorientational correlation time τ is associated with the diffusion coefficient D of the motion by the relationship [11]

$$\tau = \frac{1}{6D}. \tag{4}$$

Although this simple model is successful in explaining the dynamics in non-viscous liquids, it usually does not account for experimental observations for more complex systems, where the dynamics cannot be described by an exponential correlation function or in terms of a single correlation time [12, 13]. Therefore, when analysing the experimental results, we have also considered the spectral density functions assuming a distribution of reorientational correlation times of the form

$$J(\omega) = \int \frac{\tau g(\tau)\,\mathrm{d}\tau}{1 + (\omega\tau)^2} \tag{5}$$

where $g(\tau)$ is the distribution function. The $g(\tau)$ functions relevant for NMR experiments and their properties are discussed by Beckmann [14]. We shall not repeat his arguments, and herein give just the expression for the Davidson–Cole asymmetrical distribution [15] that has been found to fit our experimental results. For the D–C model, $g(\tau)$ takes the form

$$g(\tau) = \begin{cases} \dfrac{\sin(\pi\beta)}{\pi}\left(\dfrac{\tau}{\tau_0 - \tau}\right)^{\beta} & \text{for } 0 \leqslant \tau \leqslant \tau_0 \\ 0 & \text{for } \tau > \tau_0 \end{cases} \tag{6}$$

where τ_0 is the characteristic limiting correlation time and β is the width of the distribution, which may assume values within the range from 0 to 1. The average correlation time is defined as $\tau = \beta\tau_0$.

By substituting (6) into (5), one gets

$$J(\omega) = \frac{\sin[\beta \arctan(\omega\tau_0)]}{\omega[1 + (\omega\tau_0)^2]^{\beta/2}}. \tag{7}$$

It is seen that for $\beta = 1$ the dynamics is described by a single correlation time and equation (7) reduces to (3); on the other hand, the distribution becomes infinitely broad as β approaches 0. The width of the distribution may be related to the orientational and/or positional disorder existing in non-crystalline materials.

Adamy *et al* [5] have pointed out that in the case of molecules having chain substituents undergoing complex internal reorientations the β-parameter can serve as an indicator of molecular flexibility. The smaller the value of β, the larger the number of motions involved in the relaxation of the given interaction vector. Hence, the parameter β is expected to decrease as we go down the chain, because carbons further down are experiencing several reorientations, each with their own τ.

Quantitative interpretation of the NMR relaxation of nuclei placed in a flexible hydrocarbon chain attached to a rotating molecule is a difficult task. The problem has been considered by Wallach [1], who described such a motion in terms of an effective correlation time τ_{eff}. This time depends on the rate of the overall as well as the internal molecular motions, and on the Wigner rotation matrix elements related to the molecular structure.

In the temperature interval where the extreme-narrowing condition is valid:

$$(\omega_H + \omega_C)\tau \ll 1$$

the effective correlation time τ_{eff} for the vector connecting the directly bonded C and H atoms may be calculated from the expression [16]

$$\tau_{eff} = \frac{r_{CH}^6}{CnT_1} \tag{8}$$

where C is a constant equal to 3.56×10^{10} Å s^{-1}.

2. Experiment

Di-pentyl phthalate, $C_{18}H_{26}O_4$, whose molecular structure is shown in figure 1, is a simple glass-forming liquid. The sample studied was custom synthesized. Its purity was checked using ^{1}H and ^{13}C high-resolution NMR spectra. The sample investigated was degassed by the freeze–pump–thaw technique and sealed under vacuum in a Pyrex tube which, then, was placed in a Wilmard 10 mm o.d. tube. A deuterium source for the internal lock system was placed in the space between tubes: D_2O in the case of measurements above 273 K and $(CD_3)_2CO$ below this temperature. The relaxation times T_1 of ^{13}C were measured at a frequency of 20.3 MHz on a Tesla BS587 spectrometer equipped with an IBM computer using the inversion–recovery technique. The values of T_1 were evaluated from the magnetization recovery curves using a non-linear three-parameter fitting of line intensities [17]. To minimize the errors due to the frequency offset and the pulse length, we used a composite pulse sequence of the type

$$t_d-90°(X)-240°(Y)-90°(X)-\tau-90°-t_a \tag{9}$$

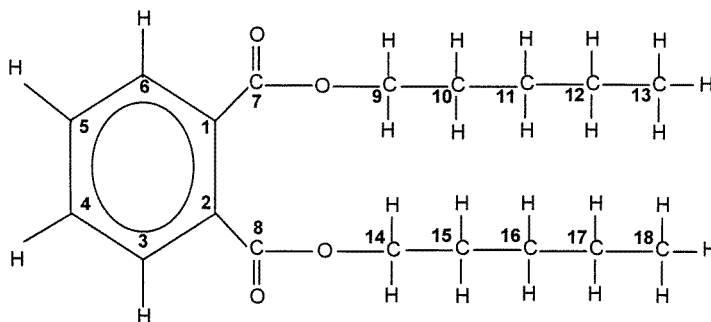where t_d is the preparation time, t_a is the acquisition time, and τ is the delay time.

Figure 1. A diagram of the DPP molecule.

The nuclear Overhauser enhancement factors were measured using the gated decoupling technique and a waiting time of at least $10T_1$ between the transients.

The temperature of the sample was controlled by a gas-flow cryostat and monitored with an accuracy of 1 K. To allow the sample to reach thermal equilibrium, it was kept at a given temperature for 30 min before the data collection.

3. Results and discussion

The natural-abundance ^{13}C NMR spectrum of liquid DPP registered at room temperature is shown in figure 2. The chemical shift assignments are given in table 1. The resolution obtained
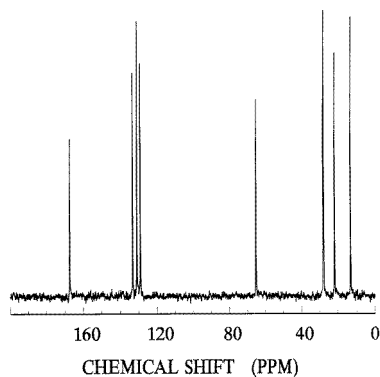
Figure 2. The ^{13}C NMR spectrum of liquid DPP registered at room temperature.

Table 1. ^{13}C chemical shift assignment in DPP.

Carbon No	Chemical shift (ppm) relative to TMS
7, 8	157.2
1, 2	132.8
3, 6	130.7
4, 5	128.9
9, 14	65.4
10, 15	28.4
11, 16	28.2
12, 17	22.3
13, 18	13.6

makes it possible to measure T_1 precisely for all individual carbons in DPP, except for 10, 15 and 11, 16 carbons, whose resonance lines are separated by only 3.4 Hz at room temperature and overlap at lower temperatures. In this paper we use the spectral lines due to 3, 6 and 4, 5 benzene ring carbons to probe the overall molecular dynamics and lines due to 9, 14; 10, 15; 11, 16; 12, 17; 13, 18 chain carbons to probe directly the internal dynamics of the chain substituents. We have left out 1, 2 and 7, 8 carbons which are not directly bonded to hydrogen atoms and therefore feature a very long relaxation time. The measured values of nT_1 are plotted versus $1000/T$ in figure 3.

It is seen that the relaxation behaviour of the ring carbons is similar and shows a distinct minimum of about 45 ms at 256.5 K. In the case of the chain carbons the minima are much less pronounced, and for some of carbons they do not show at all.

Figure 4 depicts the behaviour of the NOE factors plotted versus $1000/T$. In the highest-temperature region the NOE is constant at about 3, for all carbons studied. This value reduces as the temperature of the sample is lowered to about 1.35 for the ring carbons. For the chain carbons the degree of reduction is lower and it depends on the position of the carbon in the alkyl chain.

We attempted to explain the experimental results using the single-correlation-time model and assuming a functional form of this time given by the Arrhenius equation:

$$\tau = \tau_0 \exp(E/RT). \tag{10}$$

The analysis consisted in substituting equation (10) into equation (3) and the use of the resulting spectral density function in equations (1) and (2). It is not surprising that this simple model
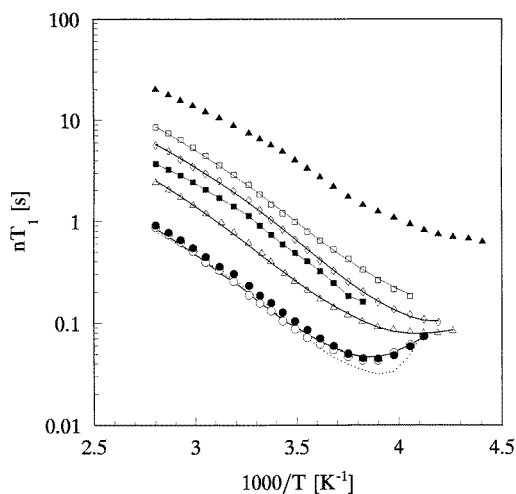
Figure 3. nT_1 for chemically non-equivalent carbons in DPP versus inverse temperature; carbons 4, 5: open circles; carbons 3, 6: full circles; carbons 9, 14: open triangles; carbons 10, 15: full squares; carbons 11, 16: rhombi; carbons 12, 17: squares; carbons 13, 18: full triangles; dotted line: BPP model and an Arrhenius dependence of the correlation time; solid line: D–C model and τ following the Vogel–Fulcher formula.
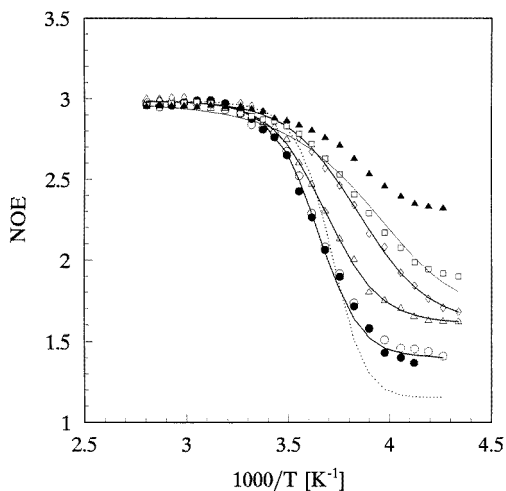

Figure 4. NOE factors of chemically non-equivalent carbons in DPP versus inverse temperature: carbons 4, 5: open circles; carbons 3, 6: full circles; carbons 9, 14: open triangles; carbons 11, 16: rhombi; carbons 12, 17: squares; carbons 13, 18: full triangles; dotted line: BPP model and an Arrhenius dependence of the correlation time; solid line: D–C model and τ following the Vogel–Fulcher formula.

failed to describe the relaxation behaviour of either the ring or the chain carbons in this complex molecule, featuring asymmetric shape and a high degree of internal mobility.

Then we attempted to analyse the data assuming a single-exponential correlation function and the temperature dependence of τ following the Vogel–Fulcher behaviour [8]:

$$\tau = a \exp B/(T - T_0) \tag{11}$$

where the Vogel temperature T_0 corresponds to the limit at which τ becomes infinite. Such a dependence is able to describe the dramatic increase of the timescale for the molecular motion, which is observed as the temperature of a supercooled liquid is lowered. When $T_0 = 0$ the Arrhenius equation results, and $B = E/k$.

The results calculated for the ring carbons 3 and 6 are shown by the dotted curves in figures 3 and 4. It is seen that the agreement between the theory and the experiment is not quite satisfactory, especially in the low-temperature region. For the chain carbons the fit based on the single-correlation-time model does not account for the experiment at all; therefore we do not show the respective calculated results in the figures.
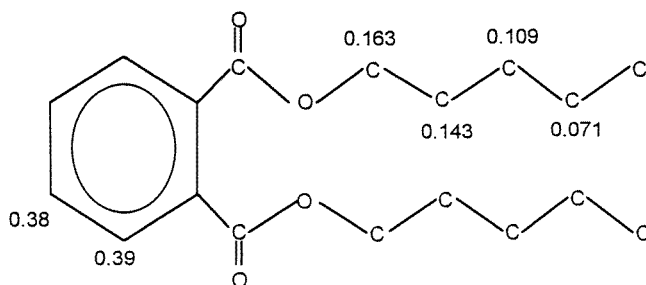

Figure 5. The distribution parameter β of the specific carbon atoms in DPP.

We have found that the experimental T_1-results can be successfully explained in terms of the asymmetric Davidson–Cole distribution function. The best fit of equations (1), (7), (11) to the experimental T_1-values is shown by solid lines in figure 3. As a check of the validity of the model adopted, we have used the optimized parameters of the nT_1-fit to reproduce the experimental NOE values. The temperature dependence of the calculated NOE factors is shown using solid lines in figure 4. It is seen that the Davidson–Cole distribution represents the NOE factors as well as it does the ^{13}C nT_1-data. The values of β for the specific chemically non-equivalent carbons are shown in figure 5. The β-values of the ring carbons are within experimental error the same, which implies that the overall motion in DPP may be considered as isotropic. The distribution parameter β decreases as the position of the carbon atom approaches
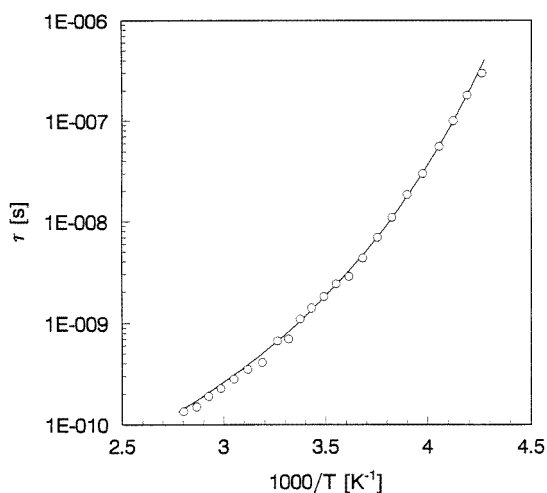

Figure 6. The dependence of the overall correlation time in DPP versus inverse temperature; the solid line is the fit of equation (11) to experimental data.

the end of the chain. If, as suggested by Adamy *et al* [5], β is indicative of the mobility gradient, then it is seen that the mobility of the chains in DPP increases as one moves towards their ends. The β-parameter of the ring carbons was used to derive from the measured relaxation curves the temperature dependence of the correlation time characterizing overall molecular motion shown in figure 6. It is apparent that in the temperature interval studied this dependence does not follow the Arrhenius behaviour. Instead we were able to it to equation (11). The solid line in figure 6 representing the best fit yields the following parameters: $a = 2.185 \times 10^{-12}$ s, $B = 784.75$ K, and $T_0 = 169.33$ K.
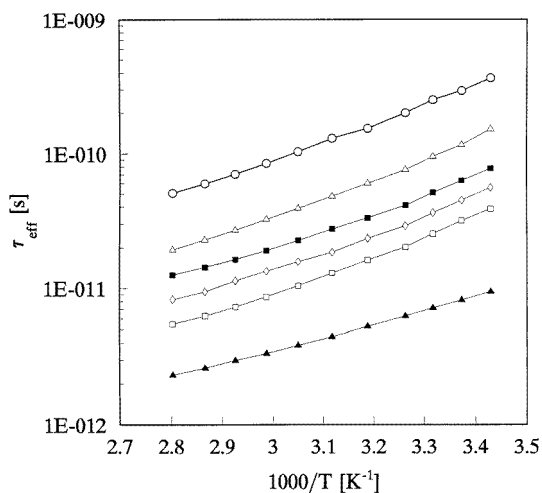

Figure 7. Effective correlation times of individual carbon atoms in DPP versus inverse temperature; carbons 4; 5: open circles, carbons 9, 14: open triangles; carbons 10, 15: full squares; carbons 11, 16: rhombi; carbons 12, 17: squares; carbons 13, 18: full triangles.
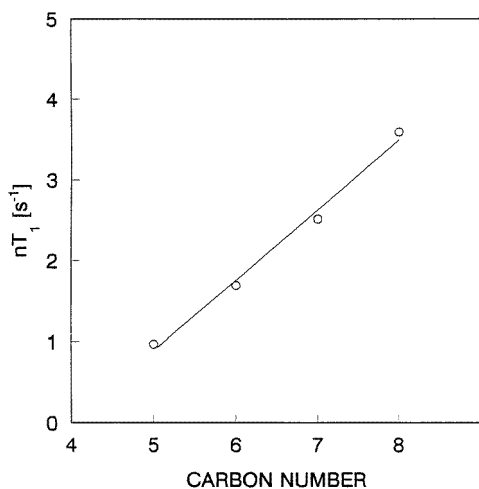

Figure 8. The dependence of nT_1 for chain carbons in DPP at 324 K.

Since the experimental data presented in this paper cover both motionally narrowed as well as slow-motion regions, we tested the statement concerning the chain dynamics using τ_{eff} derived from the high-temperature relaxation data. The values of the τ_{eff} obtained using experimental data and equation (8) plotted in figure 7 show that the effective correlation time is the shortest for the motion of the methyl group and increases as one moves along the chain towards the ring. The overall correlation time and τ_{eff} characterizing reorientations around

consecutive C–C bonds show similar temperature dependences. Such a behaviour points to the existence of multiple internal reorientations occurring at a rate faster than the overall molecular rotation [1]. To evaluate the relative mobility of the consecutive chain carbons, we plotted in figure 8 the dependence of nT_1 versus carbon number. According to the model for multiple internal reorientations [2], the linear dependence observed is consistent with equal rotational diffusion constants for all internal bonds considered.

4. Summary

The study shows that the dynamics in DPP can be successfully explained in terms of the Davidson–Cole model involving an asymmetrical distribution of correlation times. The functional form of this time shows the Vogel–Fulcher behaviour. The distribution parameters β of the successive chemically non-equivalent carbons reflect the mobility gradient existing along the alkyl chains in DPP. This conclusion is supported by the analysis of τ_{eff} derived from the high-temperature relaxation data.

References

 [1] Wallach D 1967 *J. Chem. Phys.* **47** 5258
 [2] Levine Y K, Partington P and Roberts G C K 1973 *Mol. Phys.* **25** 497
 [3] Daragan V A and Mayo K H 1998 *J. Magn. Reson.* **130** 329
 [4] Wright D A, Axelson D E and Levy G C 1979 *Topics in Carbon-13 NMR* vol 3, ed G C Levy (New York: Wiley)
 [5] Adamy S T, Garndinetti P J, Masuda G, Campbell O and Jonas J 1991 *J. Chem. Phys.* **94** 3568
 [6] Bratt P J, Gillies D G, Sutcliffe L H and Williams A J 1990 *J. Phys. Chem.* **94** 2727
 [7] Szczesniak E, Glowinkowski S, Suchanski W and Jurga S 1997 *Solid State Nucl. Magn. Reson.* **8** 73
 [8] Fujara F, Geil B, Silescu H and Fleischer G 1992 *Z. Phys.* B **88** 195
 [9] Heatley F 1979 *Prog. Nucl. Magn. Reson. Spectrosc.* **13** 47
[10] Bloembergen N, Purcell E M and Pound R V 1948 *Phys. Rev.* **73** 679
[11] Boere R T and Kidd R G 1982 *Annu. Rep. NMR Spectrosc.* **13** 319
[12] Glowinkowski S, Jurga S, Suchanski W and Szczesniak E 1997 *Solid State Nucl. Magn. Reson.* **7** 313
[13] Suchanski W, Szczesniak E and Jurga S 1998 *J. Phys.: Condens. Matter* **10** 6243
[14] Beckmann P A 1988 *Phys. Rep.* **171** 85
[15] Davidson D W and Cole R H 1951 *J. Chem. Phys.* **19** 1484
[16] Jonas J, Adamy S T, Grandinetti P J, Masuda Y, Morris S J, Campbell D M and Li Y 1989 *J. Phys. Chem.* **94** 1157
[17] Kowalewski J, Levy G C, Johnson L and Palmer L I 1977 *J. Magn. Reson.* **26** 533